Modeling Noise Effects in Time-to-Digital Converters

Pasquale Napolitano, Antonio Moschitta, Paolo Carbone

University of Perugia, DIEI – Via G. Duranti, 93 - 06125 Perugia, Italy
phone: +390755853933 - fax:+390755853654
e-mail: {pasquale.napolitano,antonio.moschitta,paolo.carbone}@diei.unipg.it

Abstract **-** In this work, the main sources of error affecting time interval measurements are analyzed and modeled. Time interpolation techniques utilizing both synchronous and asynchronous strategies to perform time measurements have been considered. Jitter on start and stop timing signals, interpolator nonlinearities, quantization error and jitter affecting the system clock driving the counter have been recognized as the main contributors to measurement uncertainty and their effects are analytically described. A deeper investigation on the cumulative effect of the clock jitter is discussed in order to determine mean values, variances and probability density functions of quantizer output and quantization error sequences. Simulations showing mean values and variances of the quantizer output are also presented, in order to validate theoretical results. The obtained model is useful both for design and testing purposes.
Index Terms - Time-to-Digital Converter (TDC); Uncertainty Analysis; Error Analysis.

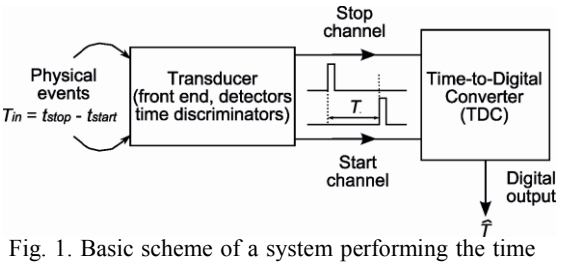

Fig. 1. Basic scheme of a system performing the time interval measurements by means of a TDC [1].

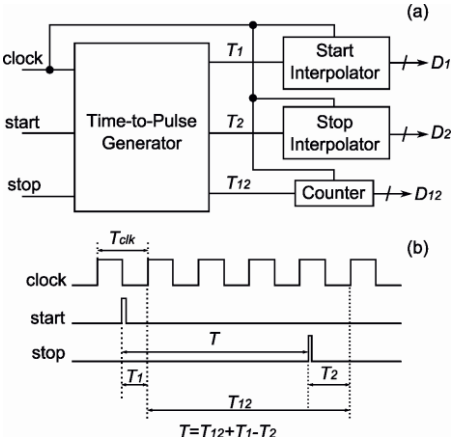

Fig. 2. Scheme (a) and timing diagram (b) of an interpolating TDC [1], [2].

I. Introduction

Time-to-Digital Converters (TDCs) are electronic devices utilized for the conversion of time intervals into digital words. Their usage spreads into several fields of application, such as scientific and research activities, medical applications, security and surveying, industrial processes [1].
The basic scheme of a system performing time measurements is shown in Fig. 1. Two physical events, occurring at $t=t_{start}$ and $t=t_{stop}$ respectively, are first transduced into two electrical pulses. Then these pulses are applied to the TDC start and stop channels, defining the duration of the incoming interval T. Finally, this time interval is digitized by the TDC.
The electrical pulses are generated by a transducer, which is the main responsible for the determination of the time instants. In fact, any uncertainty in the definition of these instants mirrors into accuracy limitations. Other sources of uncertainty may affect the time-to-digital conversion, depending on the utilized architecture and exploited technology. An interpolating TDC is considered in this paper, whose basic scheme and timing diagrams are shown in Fig. 2. Interpolation methods, combining the advantages of analog and digital methods, achieve fine resolution over a wide measurement range, thus representing one of the most widely employed time measurement technique [3], [4]. In this case, as shown in Fig. 2(a), a time-to-pulse generator decomposes T into three parts, separately digitized. In particular, fine interpolators digitize T_1 into D_1 and T_2 into D_2, while a counter provides the digital representation D_{12} of T_{12}. In order to obtain good linearity over a wide range, a stable clock

signal *clk* must be used to drive the counter, while the usage of fine interpolators improves resolution. Further details concerning the most commonly used interpolator architectures can be found in [1].
The strategy adopted for time measurements is asynchronous if the start and stop events are unsynchronized in time with *clk*. Otherwise, if the start or the stop events are synchronized with *clk*, the time measurement is synchronous [5], and may be performed by exploiting just one interpolator [1].

II. Synchronous and asynchronous TDC operating principles

In this section, the TDC is assumed to be ideally noise-free and the quantization error sequence e_q is defined and analytically described. At first an asynchronous interpolating TDC is considered. For a fixed incoming interval T, T_1 is a random variable uniformly distributed within a clock period T_c, while T_2 and T_{12} are correlated in time with T_1 [5]. Assuming each fine interpolator to be an ideal b-bit resolution truncation quantizer, the digitized time interval $\hat{T}$ can be expressed as:

$$\hat{T} = D_{12}T_c + (D_1 - D_2)\delta, \tag{1}$$

where D_1, D_2 and D_{12} are the digital representations of T_1, T_2 and T_{12} respectively and $\delta = T_c/2^b$ is the TDC quantization step. By defining $T_q = \lfloor T/T_c \rfloor$ and $\varepsilon_q = \langle T/T_c \rangle$, where $\lfloor \cdot \rfloor$ is the integer floor operator and $\langle \cdot \rangle$ is the fractional part operator, it can easily be shown that the quantization error can be expressed as:

$$e_q = \hat{T} - T = (D_1\delta - T_1) - (D_2\delta - T_2) = \begin{cases} \delta(1-\eta), & \left\langle \frac{T_1}{\delta} \right\rangle < \eta \\ -\delta\eta, & \left\langle \frac{T_1}{\delta} \right\rangle \geq \eta \end{cases}, \tag{2}$$

where $\eta = \langle \varepsilon_q T_c / \delta \rangle$.

Since T_1 is a random variable and e_q is a deterministic function of T_1, e_q becomes a random variable that may assume two possible values depending on ε_q, that differ by δ. Thus, the asynchronous interpolating TDC error e_q has a binomial distribution, similarly to the asynchronous counter method [1], [5], [6]. From (2) and by assuming T_1 uniformly distributed in [0, T_c), it can be proven that e_q has a zero mean value and the following standard deviation:

$$\sigma_q = \delta\sqrt{\eta(1-\eta)}. \tag{3}$$

If a synchronous interpolating TDC is considered, for a fixed value of T, e_q is no longer a random variable. This may be the case in which *clk* and the start signals are synchronized in time and the counter outputs:

$$D_{12} = \left\lceil \frac{T}{T_c} \right\rceil, \tag{4}$$

where $\lceil \cdot \rceil$ is the ceil operator. A stop interpolator is then used to digitize the only time residue T_2 into D_2, improving the TDC resolution. In this case, the digitized time interval $\hat{T}$ can be derived from (1) by assuming T_1 equal to zero:

$$\hat{T} = D_{12}T_c - D_2\delta. \tag{5}$$

From (2) the quantization error is given by:

$$e_q = \hat{T} - T = T_2 - D_2\delta = \delta(1-\eta). \tag{6}$$

Because of its important role in precise time measurements, the counter method is now discussed. As stated in [5], this method utilizes a counter driven by a stable reference clock with period T_c. It provides the digital representation of T, by counting the number of periods T_c occurring between successive input signal events. The classification in synchronous and asynchronous methods still applies. Since the counter method does not use fine interpolators, its behavior can be obtained by assuming $\delta=T_c$ and $D_1=D_2=0$ in (1) through (5). More in detail, the operation of a counter asynchronously measuring T are equivalent to that of a synchronous counter measuring the time interval $T_{eq}=T-T_1$, being $T_1=T_c-\alpha$, as shown in Fig. 3. Notice that α can be modeled as a random variable uniformly distributed within a clock period. Thus, in the asynchronous case, the counter output and the quantization error are given by:

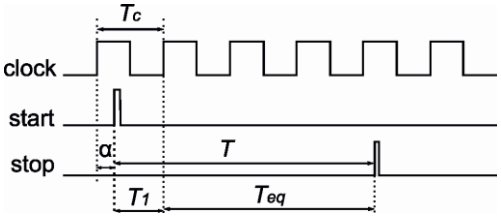

Fig. 3. Equivalent timing diagram of an asynchronous counter.

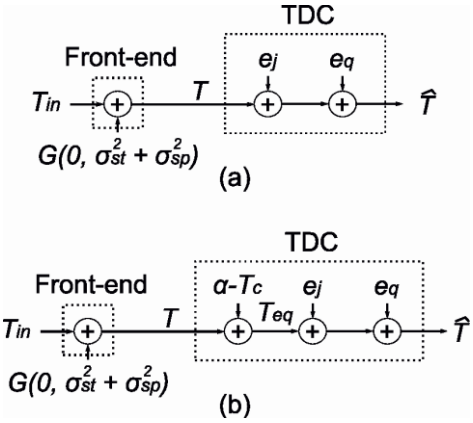

Fig. 4. Linear model for a system performing the time interval measurements by means of a synchronous (a) and asynchronous (b) counter-based TDC.

$$\hat{T} = D_{12}T_c = \left\lceil \frac{T_{eq}}{T_c} \right\rceil T_c , \tag{7}$$

$$e_q = \hat{T} - T = \begin{cases} T_c(1-\varepsilon_q), & \left\langle \frac{T_1}{T_c} \right\rangle < \varepsilon_q \\ -T_c\varepsilon_q, & \left\langle \frac{T_1}{T_c} \right\rangle \geq \varepsilon_q \end{cases} . \tag{8}$$

From (8) it follows that e_q is a zero mean random variable having a standard deviation given by:

$$\sigma_q = \delta\sqrt{\varepsilon_q(1-\varepsilon_q)} . \tag{9}$$

III. Noise in TDCs

This section focuses on the sources of uncertainty affecting time interval measurements. If a counter-based TDC is exploited, a simplified linear model of the system in Fig. 1 is represented in Fig. 4, when a synchronous or an asynchronous strategy is adopted. The TDC output can now be expressed as:

$$\hat{T} = T_{in} + error , \tag{10}$$

where Tin is the time interval to be measured, $\hat{T}$ is the measurement result, and *error* includes any source of error, both systematic and random [1], affecting the measurement process, such as quantization error, clock jitter, jitter affecting start and stop signals. These contributions are assumed to be statistically independent from each other [4]. Furthermore, because of the considerations carried out in Section II, the asynchronous counter digitizing T may be considered equivalent to a synchronous counter digitizing T_{eq}, as shown in Fig. 4.

The time discriminator has an important role in precisely determining the time instant in which a physical event occurs [7]. Thus, for each T_{in} to be measured, T is a random variable. If both the start and the stop channels are affected by additive Gaussian noise, with zero mean values and standard deviations equal to σ_{st} and σ_{sp} respectively, T is normally distributed with an expected value equal to T_{in} and a variance equal to the summation of each variance, as shown in Fig. 4. In the rest of this paper these contributions are assumed to be negligible with respect to other error contributions.

The contribution of the clock jitter $w[\cdot]$ driving the counter may become significant especially when performing long time intervals measurement, as it is cumulative. The coarse counting stops at the end of the clock rising edge following the stop pulse. Thus, ideally, the synchronous and the asynchronous counter provide $\lceil T/T_c \rceil$ and $\lceil T_{eq}/T_c \rceil$ respectively. If the clock is affected by jitter, the output may differ from the nominal value. Although more complicated models describing clock jitter exist [8], in this work it is assumed to be normally distributed with zero mean value and variance equal to σ_c^2.

Thus, the *i-th* clock period can be expressed as:

$$T_c[i] = T_c + w[i], \quad \sigma_c \ll T_c , \tag{11}$$

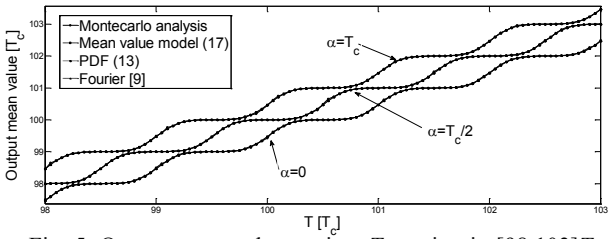

Fig. 5. Output mean value against T varying in $[98,103]T_c$, when α is equal to $\{0,\ T_c/2,\ T_c\}$. Curves obtained using Montecarlo analysis, (13), (17) and the Fourier series described in [9].

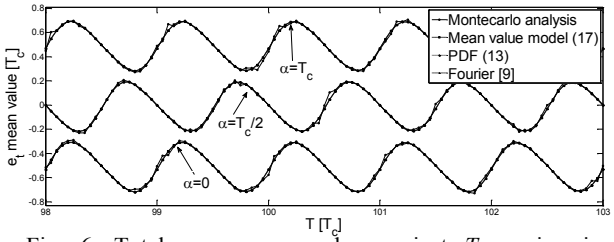

Fig. 6. Total error mean value against T varying in $[98,103]T_c$, when α is equal to $\{0,\ T_c/2,\ T_c\}$. Curves obtained using Montecarlo analysis, (13), (17) and the Fourier series described in [9].

where $w[i]$ is the i-th realization of the clock jitter. Notice that the assumption of Gaussian noise is an approximation and σ_c must be small enough to assure the clock period to always be positive, that is, $\sigma_c << T_c$. From the above considerations it follows that the N-th clock period can be expressed through a discrete-time Gaussian random walk. Thus, N clock periods end after a time given by:

$$t_N = \sum_{i=1}^{N} T_c[i] = NT_c + \sum_{i=1}^{N} w[i] \approx G\left(NT_c, N\sigma_c^2\right), \tag{12}$$

which shows the cumulative effect of clock jitter. For a given value of the random variable α, the probability to observe a certain value N at the counter output is given by:

$$P(m = N \mid \alpha) = P(t_{N-1} \le T_{eq}, t_N \ge T_{eq} \mid \alpha) = P(t_{N-1} \le T_{eq} \mid \alpha) - P(t_N \ge T_{eq} \mid \alpha) =$$
$$= \Phi\left(\frac{T_{eq} - (N-1)T_c}{\sigma_c\sqrt{N-1}}\right) - \Phi\left(\frac{T_{eq} - NT_c}{\sigma_c\sqrt{N}}\right), \tag{13}$$

where $\sigma_c << T_c$ and $\Phi(\cdot)$ is the normalized Gaussian cumulative distribution function. Notice that the synchronous case can easily be derived from (13), by assuming $\alpha = T_c$, so that $T_{eq} = T$. In practical cases, not only $\sigma_c << T_c$, but also $\sigma_c\sqrt{N} << T_c$. Thus, the counter output can be modeled as the superposition of the nominal output $D_{12}T_c$ and a $\pm T_c$ deviation, depending on the noise effects:

$$\hat{T} = T_c D_{12} + T_c i\left(e_q < -\sum_{i=1}^{D_{12}} w[i]\right) - T_c i\left(T_c - e_q < \sum_{i=1}^{D_{12}-1} w[i]\right), \tag{14}$$

where $i(\cdot)$ is the indicator function, while D_{12} and e_q have been defined in (7) and (8). Expression (14) indicates that the TDC output equals the ideal jitter-free case value given by (7) if the amplitude of the cumulative jitter is small enough. Thus, by observing that:

$$P\left(e_q < -\sum_{i=1}^{D_{12}} w[i]\right) = \Phi\left(-\frac{e_q}{D_{12}\sigma_c^2}\right) = P_1, \tag{15}$$

$$P\left(T_c - e_q < \sum_{i=1}^{D_{12}-1} w[i]\right) = \Phi\left(\frac{e_q - T_c}{(D_{12}-1)\sigma_c^2}\right) = P_2, \tag{16}$$

from (14), (15) and (16) it follows that the output mean value is given by:

$$E\left\{\hat{T}\right\} = P_0 D_{12} + P_1(D_{12} + T_c) + P_2(D_{12} - T_c) = D_{12} + T_c(P_1 - P_2), \tag{17}$$

where $P_0 = (1 - P_1 - P_2)$ is the probability of obtaining the expected count, while the output variance is:

$$\mathrm{var}\left\{\hat{T}\right\} = T_c^2(P_1 + P_2 - (P_1 - P_2)^2). \tag{18}$$

To validate (17) and (18), simulations have been carried out, by varying the TDC input T and, for a fixed value of T, by varying the offset α. Mean values and variances have been evaluated and compared with those derived from the Fourier series expansion given in [9]. Moreover, a Montecarlo analysis has been also carried out,

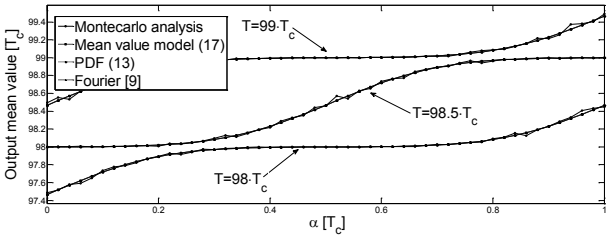

Fig. 7. Output mean value against α varying in [0, T_c], when T is equal to {98 T_c, 98.5T_c, 99 T_c}. Curves obtained using Montecarlo analysis, (13), (17) and the Fourier series described in [9].

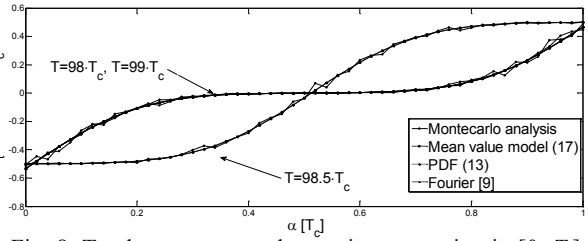

Fig. 8. Total error mean value against α varying in [0, T_c], when T is equal to {98 T_c, 98.5T_c, 99 T_c}. Curves obtained using Montecarlo analysis, (13), (17) and the Fourier series described in [9].

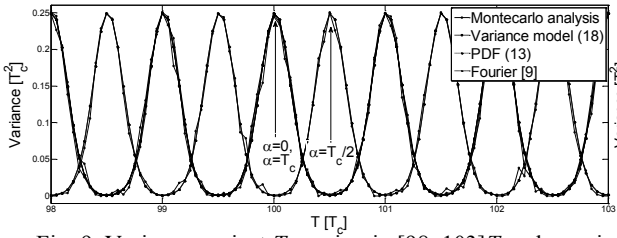

Fig. 9. Variance against T varying in [98, 103]T_c, when α is equal to {0, T_c/2, T_c}. Curves obtained using Montecarlo analysis, (13), (18) and the Fourier series described in [9].

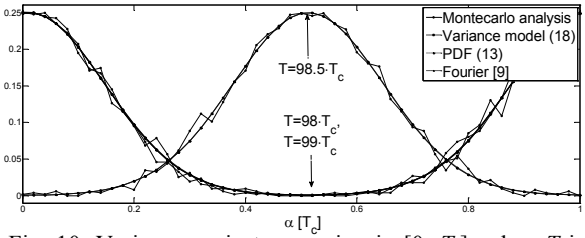

Fig. 10. Variance against α varying in [0, T_c], when T is equal to {98 T_c, 98.5T_c, 99 T_c}. Curves obtained using Montecarlo analysis, (13), (18) and the Fourier series described in [9].

considering 5000 records for each input time interval and by estimating mean values and variances. Fig. 5 and Fig. 6 show the expected value of the quantizer output and of the total error $e_t = \hat{T} - T$ against the time interval T varying between 98T_c and 103T_c, when the phase α takes values in {0, T_c/2, T_c}. The same curves are represented in Fig. 7 and Fig. 8, against α varying within T_c, when T takes values in {98, 98.5, 99}T_c. Finally, Fig. 9 and Fig. 10 show the variance of the total error and the quantizer output against T and α respectively. As these figures show, the proposed approaches to evaluate the output mean value and variance are well matched with those deriving from the Montecarlo analysis. Furthermore, for values of T much greater than T_c, the output mean value approximately becomes equal to T, because of the filtering effect of the cumulative Gaussian noise [10]. For reduced values of T, instead, the effect of Gaussian noise is reduced and the output mean value better matches the characteristic of the ideal truncation quantizer, as it is shown in Fig. 5. Moreover, the output variance is not negligible in an interval located around the quantizer transitions, the width of which increases with T. It can be shown that, if the duration of T increases, the statistical moments of interest may be derived considering only the first term of a Fourier series, as stated in [9].

IV. Conclusions

In this work, the main sources of uncertainty affecting time measurement have been investigated and discussed. The architecture of an interpolating asynchronous TDC has been considered, and further considerations concerning the synchronous strategy have been presented. Uncertainty on the determination of the start and stop timing signals, quantization error and jitter affecting the coarse counter have been recognized to be the principal responsible for the overall measurement uncertainty and have been analyzed. Because of its important role in determining the TDC performance, particular attention has been given to the jitter affecting the system clock, whose effect has been analytically defined. Simulations have been carried out by means of Matlab, proving the correctness of the theory and showing the cumulative worsening in accuracy performance with the increasing of the time interval duration. Deeper investigation on the proposed TDC architectures is needed, together with detailed models under noisy conditions, with the aim to provide a mathematical framework useful in characterization, testing and design of such devices.

Acknowledgements

This research has been supported by MIUR grant PRIN 2008TK55B55-2008.

References

[1] P. Napolitano, A. Moschitta, and P. Carbone, “A Survey on Time Interval Measurement Techniques and Testing Methods,” *I²MTC 2010, Proceedings of the 2010 International Instrumentation and Measurement Technology Conference, May 2010*, pp. 181–186.

[2] Poki Chen, Chun-Chi Chen and You-Sheng Shen, "A Low-Cost Low-Power CMOS Time-to-Digital Converter Based on Pulse Stretching," *IEEE Trans. Nucl. Sci., vol. 53, no. 4, Aug. 2006*, pp. 2215–2220.
[3] E. Räisänen-Ruotsalainen, T. Rahkonen and J. Kostamovaara, "An Integrated Time-to-Digital Converter with 30 ps Single-Shot Precision," *IEEE J. Solid-State Circuits*, vol. 35, no. 10, Oct. 2000, pp. 1507–1510.
[4] J.-P. Jansson, A. Mäntyniemi and J. Kostamovaara, "A CMOS Time-to-Digital Converter With Better Than 10 ps Single-Shot Precision," *IEEE J. Solid-State Circuits*, vol. 41, no. 6, Jun. 2006, pp. 1286–1296.
[5] Józef Kalisz, "Review of methods for time interval measurements with picosecond resolution," *Metrologia*, 41, 2004, pp. 17–32.
[6] Hewlett-Packard Application Note 162-1, "Time Interval Averaging".
[7] I. Nissinen, J. Kostamovaara, "On-Chip Voltage Reference-Based Time to-Digital Converter for Pulsed Time-of-Flight Laser Radar Measurements," *IEEE Trans. on Instrumentation and Measurement*, VOL. 58, NO. 6, June 2009, pp. 1938–1948.
[8] S. S. Awad, "Analysis of Accumulated Timing-Jitter in the Time Domain," *IEEE Trans. on Instrumentation and Measurement*, VOL. 47, NO. 1, Feb. 1998, pp. 69–73.
[9] P. Carbone, D. Petri, "Mean Value and Variance of Noisy Quantized Data," *Measurement*, Vol. 23, Number 3, Apr. 1998, pp. 131–144(14).
[10] P. Carbone, "Quantitative Criteria for the Design of Dither-Based Quantizing Systems," *IEEE Trans. on Instrumentation and Measurement*, VOL. 46, Issue 3, Jun. 1997, pp. 656–659.